

Alma Mater Studiorum Università di Bologna  
Archivio istituzionale della ricerca

Could hypoxia influence basic biological properties and ultrastructural features of adult canine mesenchymal stem /stromal cells?

This is the final peer-reviewed author's accepted manuscript (postprint) of the following publication:

*Published Version:*

Iacono, E., Pascucci, L., Bazzucchi, C., Cunto, M., Ricci, F., Rossi, B., et al. (2018). Could hypoxia influence basic biological properties and ultrastructural features of adult canine mesenchymal stem /stromal cells?. VETERINARY RESEARCH COMMUNICATIONS, 42(4), 297-308 [10.1007/s11259-018-9738-9].

*Availability:*

This version is available at: <https://hdl.handle.net/11585/649006> since: 2019-02-12

*Published:*

DOI: <http://doi.org/10.1007/s11259-018-9738-9>

*Terms of use:*

Some rights reserved. The terms and conditions for the reuse of this version of the manuscript are specified in the publishing policy. For all terms of use and more information see the publisher's website.

This item was downloaded from IRIS Università di Bologna (<https://cris.unibo.it/>).  
When citing, please refer to the published version.

(Article begins on next page)

1  
2  
3  
4 “This is a post-peer-review, pre-copyedit version of an article published in  
5 Veterinary Research Communications. The final authenticated version is  
6 available online at: <http://dx.doi.org/10.1007/s11259-018-9738-9>.

7  
8  
9  
10 This version is subjected to Springer Nature terms for reuse that can be found at:  
11 <https://www.springer.com/gp/open-access/authors-rights/aam-terms-v1>  
12  
13

**Could hypoxia influence basic biological properties and ultrastructural features of adult canine mesenchymal stem /stromal cells?**

Eleonora Iacono<sup>1\*</sup>, 0000-0002-4435-1844

Luisa Pascucci<sup>2</sup>, 0000-0002-2562-1140

Cinzia Bazzucchi<sup>2</sup>

Marco Cunto<sup>1</sup>, 0000-0002-2562-1140

Francesca Ricci<sup>3</sup>

Barbara Rossi<sup>1</sup>

Barbara Merlo<sup>1</sup>, 0000-0001-7029-5404

<sup>1</sup>Department of Veterinary Medical Sciences, University of Bologna, Italy, via Tolara di Sopra 50, 40064, Ozzano Emilia (Bologna), Italy

<sup>2</sup>Department of Veterinary Medicine, University of Perugia, via San Costanzo 4, 06126, Perugia, Italy

<sup>3</sup>Immunohaematology and Transfusion Medicine, S.Orsola-Malpighi Hospital, Bologna, Italy

\*Corresponding to: Prof. Eleonora Iacono: <sup>1</sup>Department of Veterinary Medical Sciences, University of Bologna, Italy, via Tolara di Sopra 50, 40064, Ozzano Emilia (Bologna), Italy.

E-mail: [eleonora.iacono2@unibo.it](mailto:eleonora.iacono2@unibo.it).

Phone number: +39-0512097567.

**Acknowledgements**

The Authors thank Prof. Daniele Zambelli, and Dr. Giulia Ballotta, Department of Veterinary Medical Sciences, University of Bologna, for the help given in samples recovery.

## **Abstract**

The aim of the present study was to compare canine adipose tissue mesenchymal stem cells cultured under normoxic (20% O<sub>2</sub>) and not severe hypoxic (7% O<sub>2</sub>) conditions in terms of marker expression, proliferation rate, differentiation potential and cell morphology. Intra-abdominal fat tissue samples were recovered from 4 dogs and cells isolated from each sample were cultured under hypoxic and normoxic conditions. Proliferation rate and adhesion ability were determined, differentiation towards chondrogenic, osteogenic and adipogenic lineages was induced; the expression of CD44, CD34, DLA-DQA1, DLA-DRA1 was determined by PCR, while flow cytometry analysis for CD90, CD105, CD45 and CD14 was carried out. The morphological study was performed by transmission electron microscopy. Canine AT-MSCs, cultured under different oxygen tensions, maintained their basic biological features. However, under hypoxia, cells were not able to form spheroid aggregates revealing a reduction of their adhesiveness. In both conditions, MSCs mainly displayed the same ultrastructural morphology and retained the ability to produce membrane vesicles. Noteworthy, MSCs cultivated under hypoxia revealed a huge shedding of large complex vesicles, containing smaller round-shaped vesicles.

In our study, hypoxia partially influences the basic biological properties and the ultrastructural features of canine mesenchymal stem /stromal cells. Further studies are needed to clarify how hypoxia affects EVs production in term of amount and content in order to understand its contribution in tissue regenerative mechanisms and the possible employment in clinical applications. The findings of the present work could be noteworthy for canine as well as for other mammalian species.

## **Key words**

canine, mesenchymal stem cells, hypoxia, electron microscopy

## 1. Introduction

Naturally occurring diseases in companion animals, such as *Canis familiaris*, can be suitable models for human genetic and acquired diseases, helping to define the potential therapeutic efficiency and safety of stem cells therapy (Hayes et al., 2008; Schneider et al., 2008).

Furthermore, the effective management of companion animals, such as dog, for their owners requires sophisticated new treatments and preventive strategies. Mesenchymal stem/stromal cells are the most promising candidates for tissue engineering and regenerative medicine applications. To date, canine derived MSCs have been established from different tissues, such as adipose tissue (Black et al., 2007), umbilical cord (Seo et al., 2009; Zucconi et al., 2010), liver and bone marrow (Wenceslau et al., 2011). Adipose tissue is ubiquitously available and has several advantages compared to other sources, particularly to bone marrow. In fact, it is easily accessible in large quantities with minimal invasive harvesting procedures. Furthermore, adipose tissue yields a high amount of MSCs (AT-MSCs) (Schäffler and Büchler, 2007).

It is known that both local injection as well as systemic administration of MSCs result in the successful engraftment of a small percentage of the injected cells in the site of the injury (Chimenti et al., 2016). Consistent with these findings, some studies recently showed that the regenerative ability of MSCs could be mainly attributed to the production of molecules and mediators capable of activating the intrinsic regenerative process in the damaged tissues inhibiting apoptosis and fibrosis, enhancing angiogenesis, stimulating mitosis and/or differentiation of tissue-resident progenitor cells, and modulating the immune response (Lange-Consiglio et al., 2016). These bioactive factors are freely secreted in the extracellular environment or are enclosed in micrometric and nanometric vesicles (EVs) that are released from MSCs (Yagi et al., 2010; Liang et al., 2014). They enclose lipids, growth factors, cytokines and different kinds of RNAs that are important mediators of cell- to-cell

89 communication (Huang et al., 2013; Pascucci et al., 2014a; Pascucci et al., 2015; Crivelli et  
90 al., 2017). EVs payload and their surface markers are strictly related to cell parent lineage and  
91 are influenced by cell metabolic state during their biogenesis (Tetta et al., 2013). For these  
92 reasons, EVs have a double role in physiological and pathological conditions, equally  
93 contributing to suppress or support a pathological condition (Chaput et al., 2011), depending  
94 on whether they are “good or bad” vesicles (Lo Cicero et al., 2015). Moreover, EVs exhibit  
95 many of the superficial markers, cytokines, growth factors and the immune modulatory  
96 properties of their origin cells (Gyorgy et al., 2015). Therefore, EVs could be used as smaller  
97 cellular “alter ego”, in order to achieve innovative cell-free strategies (Gyorgy et al., 2015).  
98 Furthermore, because of their capacity to encapsulate both hydrophilic and lipophilic  
99 molecules and to deliver them, EVs from MSCs could be considered as drug delivery systems  
100 (Bonomi et al., 2017; Pascucci et al., 2014b).

101 Several Authors reported the ultrastructural features and EVs production by adult and foetal  
102 human (Budoni et al., 2013; Del Fattore et al., 2015) and equine MSCs (Pascucci et al.,  
103 2014a; Pascucci et al., 2015; Lange-Consiglio et al., 2016; Iacono et al., 2017) and their  
104 possible therapeutic applications (Budoni et al., 2013; Lange-Consiglio et al., 2016; Iacono et  
105 al., 2017). Only one study briefly described the appearance, at transmission electron  
106 microscopy, of canine bone marrow MSCs (Bonomi et al., 2017), but the EVs production by  
107 these cells was no mentioned.

108 MSCs migration towards the injured tissue increases under hypoxic conditions because low  
109 oxygen tension changes their surface receptors and the interaction with the damage tissue,  
110 even if it is strictly related to MSCs close to the injured site (Annabi et al., 2003). Moreover,  
111 AT-MSCs reside in a microenvironment with low oxygen tension (1-7%) and physiologically  
112 experiences an oxygen tension lower than the atmospheric tension (20-21%) (Choi et al.,  
113 2014; Choi et al., 2015). Both in humans and in dogs, MSCs are usually cultured at

atmospheric oxygen tension and the effects of hypoxia on proliferation, differentiation and molecular profiles are contradictory (Chung et al., 2012; Lee et al., 2016). No data have been reported on the effects of hypoxia on ultrastructural features and EVs production of human or animal MSCs.

The purpose of this study was to investigate cellular proliferation, differentiation potential, molecular profile, migration and adhesion ability under normoxia (21%) and hypoxia (7%). Moreover, we aimed at evaluating the ultrastructural features of canine AT-MSCs and their capacity to produce EVs in both culture conditions. We hypothesized that hypoxia (7%) could affect cellular metabolism and consequently the release of EVs.

## **2. Materials and Methods**

Chemicals were obtained from Sigma Aldrich (St. Louis, MO, USA) and laboratory plastic ware was from Sarstedt Inc. (Newton, NC, USA) and Corning (Corning, NY, USA), unless otherwise stated.

### *2.1 Animals*

Intra-abdominal fat tissue was recovered from 7 one year old bitches referred for a routine castration to the Department of Veterinary Medical Sciences, University of Bologna. The written consent was given by all owners to allow the use of removed tissue for research purposes and experimental procedures were approved by the Ethics Committee on animal use of the Department of Veterinary Medical Sciences, University of Bologna, and by the Italian Ministry of Health.

### *2.2 Samples collection and cell isolation*

Immediately after removal, AT samples were stored in DPBS supplemented with antibiotics (100 IU/ml penicillin, 100 µg/ml streptomycin) and transferred to the lab. MSCs were isolated as previously described (Iacono et al., 2015). Briefly, under a laminar flow hood, tissue was rinsed by repeated immersion in DPBS, weighed and minced finely (0.5 cm) by sterile scissors. Minced AT was transferred into a 50ml polypropylene tube and a digestion solution, containing 0.1% collagenase type I (GIBCO®, ThermoFisher Scientific, Waltham, Massachusetts, USA) dissolved in DPBS, was added (1ml solution/1g tissue) mixing thoroughly. This mix was kept in a 37°C water bath for 30 min and mixed every 10 min. After incubation, collagenase was inactivated diluting 1:1 with DPBS supplemented with 10% v/v FBS (GIBCO®, ThermoFisher Scientific, Waltham, Massachusetts, USA). The resulting solution was filtered in order to discard the undigested tissue and nucleated cells were pelleted at 470 g for 10 min. The pellet was re-suspended in culture medium [DMEM: TCM199 (GIBCO®, ThermoFisher Scientific, Waltham, Massachusetts, USA) = 1:1, plus 10% FBS]. It was centrifuged 3 times at 470 g for 10 min in order to rinse cells. Cell pellet was re-suspended in 1 ml of culture medium and cell concentration was evaluated by haemocytometer. For plating and culturing the same cell number under hypoxic and normoxic conditions, each sample was divided in 2 equal parts. The term “normoxic” indicates the standard culture conditions (humidified atmosphere with 5% CO<sub>2</sub> and 21% O<sub>2</sub>) while the term “hypoxic” is related to a humidified atmosphere with 5% CO<sub>2</sub> and 7% O<sub>2</sub>. Canine AT-MSCs cultured in normoxia will be indicated as Nor-AT-MSCs whereas the ones cultured under hypoxia will be indicated as Hyp-AT-MSCs.

### *2.3 Cell culture and population doublings*

After isolation, primary cells derived from all recovered samples were plated in a 25 cm<sup>2</sup> flask in 5 ml of culture medium at 38.5 °C under normoxic or hypoxic conditions. After 2 days of

163 in vitro culture, the medium was completely re-placed and non-adherent cells removed.  
164 Hereafter the medium was changed twice a week until adherent primary MSCs reached ~80-  
165 90% confluence and then they were dissociated by 0.25% trypsin, counted by a  
166 haemocytometer and plated at the concentration of  $5 \times 10^3$  cells/cm<sup>2</sup> as “Passage 1” (P1).  
167 Cells were allowed to proliferate until 80-90% confluence before trypsinization and  
168 successive passage.

169 Calculation of cell-doubling time (DT) and cell-doubling numbers (CD) was carried out  
170 according to the following formulae (Rainaldi et al., 1991):

171 
$$CD = \ln(N_f / N_i) / \ln(2)$$

172 where  $N_f$  and  $N_i$  are the final and the initial number of cells, respectively;

173 
$$DT = CT / CD$$

174 where CT is the cell culture time.

175

#### 176 *2.4 Adhesion and Migration Assays*

177 To define differences between Hyp-AT-MSCs and Nor-AT-MSCs, spheroid formation and  
178 migration test were performed. For each group were carried out 3 replicates for each  
179 experiment; all replicates were carried out at passage 3 of in vitro culture.

180 For adhesion assay, cells were cultured in ‘hanging drops’ (5.000 cells/drop of 25µl) for 24 h.

181 Images were acquired by a Nikon Eclipse TE 2000-U microscope. Starting from the binary  
182 masks obtained by Image J software (Processing and Analysis in Java, Version 1.6,  
183 [imagej.nih.gov/ij/](http://imagej.nih.gov/ij/)), the volume of each spheroid was computed using ReViSP  
184 ([sourceforge.net/projects/revisp](https://sourceforge.net/projects/revisp/)) (Bellotti et al., 2016), a software specifically designed to  
185 accurately estimate the volume of spheroids and to render an image of their 3D surface.

186 To assess cell migration potential, a scratch assay (also known as Wound-Healing assay) was  
187 carried out, as previously described (Liang et al., 2007). Briefly, at 80-90 % confluence the

cell monolayer was scraped using a p1000 pipet tip. After washing twice with DPBS, the dish was incubated for 24 h. Images were acquired both immediately after the tip-scratch (time 0; T0) and after the incubation period (last time point or time 1; T1), and the distances of each scratch closure were calculated by ImageJ software (Processing and Analysis in Java, Version 1.6, [imagej.nih.gov/ij/](http://imagej.nih.gov/ij/)). The migration percentages were calculated using the following formula (Rossi et al., 2014):

$$[(\text{distance at T0} - \text{distance at T1}) * 100] / \text{distance at T0}$$

## 2.5 Multilineage differentiation

*In vitro* differentiation potential of cells toward osteogenic, adipogenic and chondrogenic lineages in different culture conditions was studied. Cells ( $5 \times 10^3$  cells/cm<sup>2</sup>) were cultured under specific induction media (Table 1). As negative control, an equal number of cells was cultured in expansion medium. *In vitro* differentiation potential was assessed at passage 3 of culture in two replicates for three samples from each lineage. To cytologically evaluate differentiation, cells were fixed with 10% formalin at room temperature (RT) and stained with Oil Red O, Alcian Blue and Von Kossa for adipogenic, chondrogenic and osteogenic induction, respectively. Quantitative analysis of *in vitro* differentiation was performed by ImageJ (Processing and Analysis in Java, Version 1.6, [imagej.nih.gov/ij/](http://imagej.nih.gov/ij/)).

## 2.6 Molecular Characterization

Expression of specific MSCs (CD44), hematopoietic (CD34), and major histocompatibility complex (DLA-DQA1, DLA-DRA1) markers was investigated by PCR analysis on undifferentiated Nor-AT-MSCs and Hyp-AT-MSCs (Table 2). All tests were carried out on  $100 \times 10^3$  cells, derived from three different dogs. Experiments were performed at passage 3 of *in vitro* culture, except for DLA-DQA1 and DLA-DRA1: in fact, given the increasing demand of MSCs for clinical use also in the canine species, the expression of DLA-DQA1 and DLA-

DRA1 was also studied at P0 to assess their immunologic properties. For PCR, cells were snap-frozen and RNA was extracted using Nucleo Spin® RNA kit (Macherey-Nagel, Düren, Germany) following the manufacturer's instructions. cDNAs were synthesized by RevertAid RT Kit (ThermoFisher Scientific, Waltham, Massachusetts, USA) and used directly in PCR reactions, following the instructions of Maxima Hot Start PCR Master Mix (2X) (ThermoFisher Scientific, Waltham, Massachusetts, USA).

Canine glyceraldehyde-3-phosphate dehydrogenase (GAPDH) was employed as a reference gene in each sample in order to standardize the results and to assess RNA integrity and purity. Furthermore, for all primers, in order to assess sample purity, a RT- and a mix without primer were analyzed.

PCR products were visualized with ethidium bromide on a 2% agarose gel (Bio-Rad Laboratories, Inc., Hercules, California, USA).

## *2.7 Flow cytometry*

Cytofluorimetric analysis was carried out to study the cell surface marker expression of canine Nor-AT-MSCs and Hyp-AT-MSCs. At P3 cells were labeled with CD90, CD105, CD14, and CD45 mouse monoclonal antibodies (all from Beckman Coulter, Milan, Italy) and with isotype control mouse monoclonal antibodies. Briefly, at 80-90% of confluence, cells were harvested by trypsinization after twice rinsing with DPBS and collected at a concentration of  $10^6$  cells/ml. Fixation and permeabilization were carried out using Reagent 1 of Intraprep Kit (Beckman Coulter, Milan, Italy). Flow cytometry was performed using FC500 two-laser equipped cytometer (Beckman Coulter, Milan, Italy). Conjugated-specific antibodies or isotype-matched control mouse immunoglobulin G are listed in Table 3. Cross-reactivity of the antibodies used was screened using cultured human and canine MSCs. Incubated cells with isotype-specific IgGs were used as control cells in order to establish the

background signal. Furthermore, to verify cross-reactivity, control on circulating canine lymphocytes was carried out. The similarity of CD markers was also identified by comparing the amino acid sequences using Basic Local Alignment Search Tool (BLAST). Results were further analyzed with the CXP dedicated program.

## *2.8 Transmission Electron Microscopy (TEM)*

Ultrastructural investigation was carried out on canine Nor-AT-MSCs (n=3) and Hyp-AT-MSCs (n=3) at P3 of culture. At this time, the cells were detached from the flask by trypsin-EDTA, centrifuged at 600 g for 10 minutes to remove the medium and fixed with 2.5% glutaraldehyde in 0.1 M phosphate buffer (PB), pH 7.3, for 1 h at room temperature. They were subsequently washed twice in PB and post-fixed with 2% osmium tetroxide dissolved in 0.1 M PB, pH 7.3, for 1 h at room temperature. Cells were finally dehydrated in a graded series of ethanol up to absolute, pre-infiltrated and embedded in Epon 812 (Electron Microscopy Sciences, Hatfield, Pa, USA). Ultrathin sections (90 nm) were mounted on 200-mesh copper grids, stained with uranyl acetate and lead citrate, and examined by means of a Philips EM 208, equipped with a digital camera.

## *2.9 Statistical analysis*

CDs, DTs and percentages of migration are expressed as mean  $\pm$  standard deviation. Statistical analyses were performed using IBM SPSS Statistics 23 (IBM Corporation, Armonk, New York, USA). Data were analysed, for normal distribution, using a Shapiro-Wilk test. For growth curve, DTs and CDs were analysed using Student's T Test for paired variables. To compare single culture passage DTs one-way ANOVA and post hoc Tuckey test were applied. Data recorded from scratch test were analysed by Student's T test for paired

variables, while the 3D spheroid volumes were compared using Wilcoxon test, due to their non-normal distribution. Significance was assessed for  $P < 0.05$ .

### 3. Results

#### 3.1 Cell culture, *in vitro* differentiation and phenotype characterization

Adherent cells with the characteristic spindle-shaped morphology were isolated from all samples and cultivated both under normoxia and hypoxia condition. For all samples, in both culture conditions, undifferentiated cells were cultured until P5. At P5, total CDs registered for Nor-AT-MSCs and Hyp-AT-MSCs were not statistically different ( $12.9 \pm 3.4$  vs  $12.7 \pm 3.2$ ;  $P > 0.05$ ; Fig.1A) ( $P > 0.05$ ). No statistically significant differences ( $P > 0.05$ ) were found between total DTs in Nor-AT-MSCs and Hyp-AT-MSCs ( $3.58 \pm 2.14$  vs  $3.53 \pm 2.13$  days respectively;  $P > 0.05$ ; Fig.1B); the only difference observed was at the second passage of *in vitro* culture, when Nor-AT-MSCs DT ( $3.6 \pm 1.4$  days) was higher than Hyp-AT-MSCs DT ( $2.9 \pm 0.9$  days) (Fig.1B;  $P < 0.05$ ). Analysing DTs at different passage in the same culture group, both in Nor-AT-MSCs and Hyp-AT-MSCS a statistically significant increase was observed starting from P3 (Fig.1B;  $P < 0.05$ ).

As showed in Fig. 2A, no significant differences ( $P > 0.05$ ) in the migration abilities were observed between Nor-AT-MSCs ( $68.5 \pm 10.8$  %) and Hyp-AT-MSCs ( $76.9 \pm 10.0$  %); on the contrary, while Nor-AT-MSCs cultured in 'hanging drops' were able to form spheroids, Hyp-AT-MSCs did not form a compact spheroid (Fig.2B). For these reasons a statistically significant difference was found between spheroid volumes: the spheroid formed by Hyp-AT-MSCs was twice in volume compared to that formed by Nor-AT-MSCs ( $P < 0.05$ ).

In order to characterize canine Nor-AT-MSCs and Hyp-AT-MSCs, PCRs were performed for CD34 as hematopoietic marker, for CD44 as MSC marker, for dog leukocytes antigens DLA-DQA1 and DLA-DRA1. CD44 expression was detected in cells cultured under both

conditions, while no samples expressed CD34 (Fig.3A). DLA-DQA1 was weakly expressed only at P0, while DLA-DRA1 was not expressed by any sample, at each culture passage examined (Fig.3A).

Cells cultured under both atmosphere conditions resulted positive for mesenchymal markers CD90, and CD105. The haematopoietic markers CD14 and CD45 were expressed in low percentages (<20%) in all samples, with a significant difference ( $P<0.05$ ) in the expression of CD45 between Nor-AT-MSCs and Hyp-AT-MSCs ( $8.4 \pm 1.2$  vs  $13.0 \pm 0.5$ ) (Fig.3B).

As well as the molecular characterization seems not to be affected by *in vitro* culture conditions, also the ability of cell to differentiate *in vitro* is similar. In fact, both Nor-AT-MSCs and Hyp-AT-MSCs, cultured in induction media were able to differentiate toward osteogenic, chondrogenic and adipogenic direction (Fig.4).

### 3.2 Transmission Electron Microscopy (TEM)

When analyzed by TEM, cells cultivated in both experimental conditions were characterized by a unique euchromatic nucleus with irregular profile and one or more prominent nucleoli (Figg. 5A, 6A). Cytoplasm was populated by abundant free ribosomes. Apart from some flat profiles of RER, in both cell samples the cisternal space of the RER was often greatly distended (Figg. 5C, 6B). A consistent number of mitochondria was observed in both samples. They mostly appeared elongated and were characterized by normal cristae. Membrane integrity was maintained (Figg. 5B, 6B). Golgi apparatus was well developed and typically included flattened cisternae, transport vesicles, and heterogeneous sized vacuoles, some of which were very large and filled with either electron-lucent or fine granular material (Figg. 5B, 6C). The endo-lysosomal apparatus showed a variety of appearances; multivesicular bodies (MVBs) and endo-lysosomes were quite abundant. MVBs appeared as large vacuoles more than 500 nm in diameter containing 30 to 100 nm wide intraluminal

small vesicles. Maturation of endosomes was reflected by the progressive increasing number of intraluminal vesicles. Endo-lysosomes, on the other hand, appeared as vacuolar structures characterized by nano-vesicles, typical of late endosomes, mixed with aggregates of electron-dense material and occasional para-crystalline formations. Endo-lysosomes were present in both cell types, but they were more abundant in cells cultured under hypoxia (Figg. 5C, 5D, 6B). Autophagic vacuoles were occasionally seen in Hyp-AT-MSCs. Cellular membrane showed an irregular profile due to the presence of cytoplasmic pseudopodial evaginations and to the occurrence of large complex vesicles shedding from the cell surface. This latter phenomenon appeared more evident in Hyp-AT-MSCs where large electron-lucent vesicles frequently budded from the cell surface. These vesicles were 2000 nm or even larger in diameter and contained round-shaped 300 to 500 nm wide vesicles inside their lumen (Figg. 5F, 6E, 6F). Under both atmospheric conditions the extracellular space was populated by numerous vesicles of heterogeneous size (Figg. 5E, 6D).

#### **4. Discussion**

The use of MSCs for regenerative medicine has been proposed in human and veterinary species (Fortier and Travis, 2011). The most studied source of MSCs is bone marrow; in particular, some Authors suggested that it may be a superior source of MSCs for osteogenesis since, in this microenvironment, cells are pre-committed towards the osteogenic lineage (Noël et al., 2008). Adipose tissue is another ideal source of MSCs: it is abundant and can be easily obtained from several body's regions with minimal side effects for donor (Tapp et al., 2009). Initially, the beneficial effect of MSCs was thought to derive from their proliferation and differentiation (Kopen et al., 1999). However, the observation that only a small number of transplanted cells survive and integrate into host damaged tissue has highlighted the possibility that an alternative mechanism exists. Today, it is widespread opinion that MSCs

339 create optimal environmental conditions for tissue regeneration via a paracrine mechanism  
340 (Pascucci et al., 2014a; Crivelli et al., 2017). In particular, MSCs produce trophic factors,  
341 cytokines and signaling molecules, able to influence angiogenesis, cell proliferation,  
342 apoptosis and even recruitment of resident stem cells (Pascucci et al., 2014a). The complex  
343 interaction between MSCs and tissue microenvironment might involve both soluble factors  
344 and production of extracellular vesicles containing various molecules (György et al., 2011).  
345 The importance of tissue environmental factors, like oxygen tension, has been previously  
346 studied in human MSCs in relation to differentiation capability (Cicione et al., 2013) and cell  
347 growth (Hung et al., 2012). *In vitro*, cell cultures are generally carried out under 20-21% O<sub>2</sub>,  
348 known as normoxia, but it does not replicate the physiological or pathological hypoxia  
349 corporeal conditions (He et al., 2007). For this reason, recently many research groups have  
350 been started to compare culture and differentiation of MSCs in normoxia and hypoxia (5%  
351 O<sub>2</sub>) or severe hypoxia (1-3% O<sub>2</sub>) (Buravkova et al., 2014). Results obtained in the present  
352 study are similar to those reported previously by Chung et al. (2012) about canine AT-MSCs  
353 growth rate in normoxia (21%) and in hypoxia (7%), but different from those reported by  
354 other Authors (Lee et al., 2016). This confirms, as already reported in humans, the disparity in  
355 results obtained culturing cells under hypoxic conditions (Choi et al., 2017). Because the  
356 effects of hypoxia on proliferation rate of AT-MSCs could be influenced not only by oxygen  
357 rate but also by other different factors, such as area of body from which it was removed,  
358 different sexes and age of donor, further studies are needed to verify if this could be true also  
359 in canine species.

360 Beyond the growth curve, migration ability is an important feature of MSCs because of its  
361 fundamental significance for systemic application (Li et al., 2009; Burk et al., 2013). No  
362 differences were found between Nor-AT-MSCs and Hyp-AT-MSCs in migration ability.  
363 Since the adhesion capability is related and enhanced to differentiation potential (Pasquinelli

et al., 2007; Wang et al., 2009), in the present study, for the first time in canine species, spheroid formation *in vitro* was assessed using the hanging drop method. Cells cultured under normoxia showed a higher adhesion ability, forming smaller spheroids. However, no difference was observed in differentiation ability of cells cultured in induction medium in 21% and 7% O<sub>2</sub>. This could be related to the further reduction of oxygen within the micromasses which therefore requires a further adaptation of the cells to the new condition. As previously reported (Chung et al., 2012; Lee et al., 2016), also under our culture conditions canine AT-MSCs maintain their stemness and the characteristic molecular profile. In fact, both Nor and Hyp-AT-MSCs expressed CD44 and did not express CD34, a hematopoietic marker. Furthermore, by RT-PCR, we demonstrated that, at P3 of *in vitro* culture in normoxia and hypoxia, canine AT-MSCs did not express DLA-DRA1 and DLA-DQA1. Furthermore, as previously reported in canine MSCs (Seo et al., 2009; Filioli Urani et al., 2014), we found a very weak expression of DLA-DRA1 at P0. We could postulate that the expression of these markers has been lost during the first passages in canine AT-MSCs, confirming the low immunogenicity of these populations of cells and supporting their possible use for allo- and xenotransplantation. With the exception of a few reports, MSCs morphology has been widely disregarded in the past years (Budoni et al., 2013; Pascucci et al., 2014a; Del Fattore et al., 2015; Pascucci et al., 2015; Lange-Consiglio et al., 2016; Iacono et al., 2017). In this manuscript, we discussed the establishment of MSCs cultures from canine adipose tissue and described, for the first time, their fine structure by transmission electron microscopy. Furthermore, since also in canine species it was demonstrated that oxygen concentration is an important component of stem cell niche (Chung et al., 2012; Lee et al., 2016) but no data are present on the effects of oxygen tension on cellular components and their ability to produce EVs, we ascertained, by means of electron microscopy, that canine AT-MSCs constitutively produce EVs under different

389 oxygen tensions and we compared the effect of normoxia (21%) and hypoxia (7%) on canine  
390 AT-MSCs fine structure. The ultrastructural morphology was mainly maintained in Hyp-AT-  
391 MSCs when compared with Nor-AT-MSCs. Canine AT-MSCs were homogeneous in shape  
392 and dimensions and presented a large, irregular nucleus with multiple nucleoli, as a sign of  
393 intense metabolic activity. This was confirmed by a consistent number of mitochondria. The  
394 main differences between Hyp-AT-MSCs and Nor-AT-MSCs attained the presence of  
395 occasional autophagosomes, the increased number of endolysosomes and the abundance of  
396 large complex vesicles budding from the cell surface and containing smaller vesicles in cells  
397 cultured in 7% O<sub>2</sub>. This particular kind of EVs has never been described before in the  
398 literature in dogs, but it was frequently observed by the authors in MSCs of different species  
399 and tissue sources (Pascucci et al., 2014a; Pascucci et al., 2015). Concerning endolysosomes  
400 and autophagosomes, it could be hypothesized that the hypoxic environment could induce a  
401 mild injury because of the reduced oxygen availability, followed by the digestion of damaged  
402 cell components. Therefore, autophagy may be interpreted as a reactive behavior of the cell to  
403 the adverse environmental conditions. The increased number of large complex vesicles  
404 budding from the cell surface and containing smaller vesicles, and the great quantity of MVBs  
405 and extracellular vesicles led to hypothesize that the high metabolic and synthetic activity  
406 typical of MSCs is enhanced in Hyp-AT-MSCs respect to cells cultured in normoxia. This is  
407 supported by the presence of an unchanged synthetic apparatus formed by the euchromatic  
408 nucleus, by a great number of free ribosomes, by a well developed RER and Golgi apparatus.  
409 This last one, additionally, produce large vacuoles containing a fine granular material that  
410 could be addressed to secretion. Examination of cell monolayers by TEM, allowed to  
411 hypothesize that EVs production could be influenced by the *in vitro* culture oxygen tension.  
412 Particularly, we observed that in cells cultured under low oxygen tension, large complex EVs  
413 seems to be more numerous. As previously speculated (Pascucci et al., 2015), it is possible

that this kind of vesicles encloses smaller vesicles that, in a first phase, are grouped in specific areas, underneath the plasma membrane and are then exocytosed through an apocrine-like secretion. In this way, cells are able to package a large amount of cargo enclosed inside large complex vesicles. Even if their content needs still to be characterized, it could be speculated that it may be able to modulate, at the same time, different biological pathways so inducing a strong and polymorvous environmental response.

In equine species, it was recently demonstrated that AT-MSCs EVs are involved in modulation of different stages of angiogenesis (Pascucci et al., 2014a). Different Authors stated that hypoxia increases the secretion of angiogenic factors and that the medium conditioned by hypoxic-treated cells may enhance angiogenesis and perfusion in nude mice with ischemic hindlimbs (Rehman et al., 2004; Stubbs et al., 2012). Furthermore, hypoxic-treated cells were found to increase secretion of antitapoptotic factors, such as IL-6: this factor has been demonstrated to inhibit cardiomyocyte apoptosis and reduce infarct size (Matsushita et al., 2005; Jung et al., 2009; Przybyt et al., 2013). Recently, it was demonstrated that canine bone marrow MSCs loaded with paclitaxel (PTX) are able to release it affecting in vitro cancer cells proliferation (Bonomi et al., 2017). PTX release could be partly mediated by EVs, as previously demonstrated in an in vitro murine model. Considering that tumor environment is often characteristically hypoxic, the possible therapeutic use of MSC cultivated under hypoxia to produce EVs to be used as drug delivery system deserves a careful further study also in canine species.

The results of the present study indicate that MSCs from canine adipose tissue constitutively produce EVs that may be responsible of their paracrine activity. Furthermore, the EVs production seems to be influenced by *in vitro* culture oxygen tension. There is need for further mechanistic studies of hypoxia to elucidate its influence not only on EVs production but also in their composition in view of clinical and pharmaceutical applications.

439

440       **5. Author's declaration of interest:** No competing interests have been declared.

441

442

443

## 6. References

- Annabi B, Lee YT, Turcotte S, Naud E, Desrosiers RR, Champagne M, Eliopoulos N, Galipeau J, Béliveau R (2003) Hypoxia promotes murine bone-marrow-derived stromal cell migration and tube formation. *Stem Cells* 21:337-347. <https://doi.org/10.1634/stemcells.21-3-337>.
- Bellotti C, Duchi S, Bevilacqua A, Lucarelli E, Piccinini F (2016) Long term morphological characterization of mesenchymal stromal cells 3D spheroids built with a rapid method based on entry-level equipment. *Cytotechnology* 68:2479-2490. <https://doi.org/10.1007/s10616-016-9969-y>.
- Black LL, Gaynor J, Gahring D, Adams C, Aron D, Harman S, Gungerich DA, Harman R (2007) Effect of adipose-derived mesenchymal stem and regenerative cells on lameness in dogs with chronic osteoarthritis of the coxofemoral joints: a randomized, double-blinded, multi-center, controlled trial. *Vet Ther* 8:272-284.
- Bonomi A, Ghezzi E, Pascucci L, Aralla M, Ceserani V, Pettinari L, Coccè V, Guercio A, Alessandri G, Parati E, Brini AT, Zeira O, Pessina A (2017) Effect of canine mesenchymal stromal cells loaded with paclitaxel on growth of canine glioma and human glioblastoma cell lines. *Vet J* 223:41-47. <https://doi.org/10.1016/j.tvjl.2017.05.005>.
- Budoni M, Fierabracci A, Luciano R, Petrini S, Di Ciommo V, Muraca M (2013) The immunosuppressive effect of mesenchymal stromal cells on B lymphocytes is mediated by membrane vesicles. *Cell Transplant* 22:369-379. <https://doi.org/10.3727/096368911X582769>.
- Buravkova LB, Andreeva ER, Gogvadze V, Zhivotovsky B (2014) Mesenchymal stem cells and hypoxia: Where are we? *Mitochondrion* 19PtA:105-112. <https://doi.org/10.1016/j.mito.2014.07.005>.

467 Burk J, Ribitsch I, Gittel C, Juelke H, Kasper C, Staszuk C, Brehm W (2013) Growth and  
468 differentiation characteristics of equine mesenchymal stromal cells derived from different  
469 sources. *Vet J* 195:98-106. <https://doi.org/10.1016/j.tvjl.2012.06.004>.

470 Chaput N, Thery C (2011) Exosomes: immune properties and potential clinical  
471 implementations. *Semin Immunopathol* 33:419-440. [https://doi.org/10.1007/s00281-010-](https://doi.org/10.1007/s00281-010-0233-9)  
472 0233-9.

473 Chimenti I, Smith RR, Li TS, Gerstenblith G, Messina E, Giacomello A, Marbán E (2016)  
474 Relative roles of direct regeneration versus paracrine effects of human cardiosphere-derived  
475 cells transplanted into infarcted mice. *Circ Res* 106:971-980.  
476 <https://doi.org/10.1161/CIRCRESAHA.109.210682>.

477 Choi JR, Pingguan-Murphy B, Wan Abas WA, Yong KW, Poon CT, Noor Azmi MA, Omar  
478 SZ, Chua KH, Wan Safwani WK (2014) Impact of low oxygen tension on stemness,  
479 proliferation and differentiation potential of human adipose-derived stem cells., *Biochem*  
480 *Biophys Res Commun* 448:218-224. <https://doi.org/10.1016/j.bbrc.2014.04.096>.

481 Choi JR, Pingguan-Murphy B, Wan Abas WA, Yong KW, Poon CT, Noor Azmi MA, Omar  
482 SZ, Chua KH, Xu F, Wan Safwani WK (2015) In situ normoxia enhances survival and  
483 proliferation rate of human adipose tissue-derived stromal cells without increasing the risk of  
484 tumour genesis. *PLoS One* 10:e0115034. <https://doi.org/10.1371/journal.pone.0115034>

485 Choi JR, Yong KW, Wan Safwani WKZ (2017) Effect of hypoxia on human adipose-  
486 derived mesenchymal stem cells and its potential clinical applications. *Cell Mol Life Sci*  
487 74:2587-2600. <https://doi.org/10.1007/s00018-017-2484-2>

488 Chung DA, Hayashi K, Chrisoula A, Toupadakis CA, Wong A, Yellowley CE (2012)  
489 Osteogenic proliferation and differentiation of canine bone marrow and adipose tissue derived  
490 mesenchymal stromal cells and the influence of hypoxia. *Res Vet Sci* 92:66-75.  
491 <https://doi.org/10.1016/j.rvsc.2010.10.012>.

492 Cicione C, Muiños-López E, Hermida-Gómez T, Fuentes-Boquete I, Díaz-Prado S, Blanco FJ  
493 (2013) Effects of severe hypoxia on bone marrow mesenchymal stem cells differentiation  
494 potential. *Stem Cells Int*:232896. <http://dx.doi.org/10.1155/2013/232896>.

495 Crivelli B, Chlapanidas T, Perteghella S, Lucarelli E, Pascucci L, Brini AT, Ferrero I,  
496 Marazzi M, Pessina A, Torre ML (2017) Mesenchymal stem/stromal cell extracellular  
497 vesicles: From active principle to next generation drug delivery system. *J Control Release*  
498 262:104-117. <https://doi.org/10.1016/j.jconrel.2017.07.023>.

499 Del Fattore A, Luciano R, Pascucci L, Goffredo BM, Giorda E, Scapaticci M, Fierabracci A,  
500 Muraca M (2015) Immunoregulatory effects of mesenchymal stem cell-derived extracellular  
501 vesicles on T lymphocytes. *Cell Transplant* 24:2615-2627.  
502 <https://doi.org/10.3727/096368915X687543>.

503 Filioli Uranio M, Dell'Aquila ME, Caira M, Guaricci AC, Ventura M, Catacchio CR, Ventura  
504 M, Cremonesi F (2014) Characterization and in vitro differentiation potency of early-passage  
505 canine amnion- and umbilical cord-derived mesenchymal stem cells as related to gestational  
506 age. *Mol Reprod Dev* 81:539-551. <https://doi.org/10.1002/mrd.21311>.

507 Fortier LA, Travis AJ (2011) Stem cells in veterinary medicine. *Stem Cell Res Ther* 2:9.  
508 <https://doi.org/10.1186/scrt50>

509 Gyorgy B, Hung ME, Breakefield XO (2015) Therapeutic applications of extracellular  
510 vesicles: clinical promise and open questions. *Ann Rev Pharmacol Toxicol* 55:439-464.

511 Hayes B, Fagerlie SR, Ramakrishnan A, Baran S, Harkey M, Graf L, Bar M, Bendoraite A,  
512 Tewari M, Torok-Storb B (2008) Derivation, characterization, and in vitro differentiation of  
513 canine embryonic stem cells. *Stem Cells* 26:465-473. [https://doi.org/10.1634/stemcells.2007-](https://doi.org/10.1634/stemcells.2007-0640)  
514 0640.

515 He MC, Li J, Zhao CH (2007) Effect of hypoxia on mesenchymal stem cells - review. *J Exp*  
516 *Hematol Chinese Ass Pathophys* 15:433-436.

517 Huang YC, Parolini O, Deng L (2013) The potential role of microvesicles in mesenchymal  
 518 stem cell-based therapy. *Stem Cells Dev* 15:841-844. <https://doi.org/10.1089/scd.2012.0631>.  
 519 Hung SP, Ho JH, Shih YR, Lo T, Lee OK (2012) Hypoxia promotes proliferation and  
 520 osteogenic differentiation potentials of human mesenchymal stem cells. *J Orthop Res* 30:260-  
 521 266. <https://doi.org/10.1002/jor.21517>.  
 522 Iacono E, Merlo B, Romagnoli N, Rossi B, Ricci F, Spadari A (2015) Equine Bone Marrow  
 523 and Adipose Tissue Mesenchymal Stem Cells: Cytofluorimetric Characterization, In Vitro  
 524 Differentiation, and Clinical Application. *J Eq Vet Sci* 35:130-140.  
 525 <https://doi.org/10.1016/j.jevs.2014.12.010>.  
 526 Iacono E, Pascucci L, Rossi B, Bazzucchi C, Lanci A, Ceccoli M, Merlo B (2017)  
 527 Ultrastructural characteristics and immune profile of equine MSCs from fetal adnexa.  
 528 *Reproduction* 154:509-519. <https://doi.org/10.1530/REP-17-0032>.  
 529 Jung DI, Ha J, Kang BT, Kim JW, Quan FS, Lee JH, Woo EJ, Park HM (2009) A comparison  
 530 of autologous and allogenic bone marrow-derived mesenchymal stem cell transplantation in  
 531 canine spinal cord injury. *J Neurol Sci* 285:67-77. <https://doi.org/10.1016/j.jns.2009.05.027>.  
 532 Kopen GC, Prockop DJ, Phinney DG (1999) Marrow stromal cells migrate throughout  
 533 forebrain and cerebellum, and they differentiate into astrocytes after injection into neonatal  
 534 mouse brains. *Proc Nat Acad Sci U S A* 96:10711-10716.  
 535 <https://doi.org/10.1073/pnas.96.19.10711>.  
 536 Lange-Consiglio A, Perrini C, Tasquier R, Deregibus MC, Camussi G, Pascucci L, Marini  
 537 MG, Corradetti B, Bizzaro D, De Vita B, Romele P, Parolini O, Cremonesi F (2016) Equine  
 538 Amniotic Microvesicles and Their Anti-Inflammatory Potential in a Tenocyte Model In Vitro.  
 539 *Stem Cells Dev* 25:610-621. <https://doi.org/10.1089/scd.2015.0348>.

540 Lee J, Byeon JS, Lee KS, Gu NY, Lee GB, Kim HR, Cho IS, Cha SH (2016) Chondrogenic  
541 potential and anti-senescence effect of hypoxia on canine adipose mesenchymal stem cells.  
542 Vet Res Commun 40:1-10. <https://doi.org/10.1007/s11259-015-9647-0>.

543 Li G, Zhang X, Wang H, Wang X, Meng CL, Chan CY, Yew DT, Tsang KS, Li K, Tsai SN,  
544 Ngai SM, Han ZC, Lin MC, He ML, Kung HF (2009) Comparative proteomic analysis of  
545 mesenchymal stem cells derived from human bone marrow, umbilical cord and placenta:  
546 implication in the migration. Proteomics 9:20-30. <https://doi.org/10.1002/pmic.200701195>.

547 Liang CC, Park AY, Guan JL (2007) In vitro scratch assay: a convenient and inexpensive  
548 method for analysis of cell migration in vitro. Nat Protoc 2:329-333.  
549 <https://doi.org/10.1038/nprot.2007.30>.

550 Liang X, Ding Y, Zhang Y, Tse FT, Lian Q (2014) Paracrine mechanisms of mesenchymal  
551 stem cell-based therapy: current status and perspectives. Cell Transplant 23:1045-1059.  
552 <https://doi.org/10.3727/096368913X667709>.

553 Lo Cicero A, Stahl PD, Raposo G (2015) Extracellular vesicles shuffling intercellular  
554 messages: for good or for bad. Curr Opin Cell Biol 35:69-77.  
555 <https://doi.org/10.1016/j.ceb.2015.04.013>.

556 Matsushita K, Iwanaga S, Oda T, Kimura K, Shimada M, Sano M, Umezawa A, Hata J,  
557 Ogawa S (2005) Interleukin-6/soluble interleukin-6 receptor complex reduces infarct size via  
558 inhibiting myocardial apoptosis. Lab Invest 85:1210-1223.  
559 <https://doi.org/10.1038/labinvest.3700322>.

560 Noël D, Caton D, Roche S, Bony C, Lehmann S, Casteilla L, Jorgensen C, Cousin B (2008)  
561 Cell specific differences between human adipose-derived and mesenchymal-stromal cells  
562 despite similar differentiation potentials. Exp Cell Res 314:1575-1584.  
563 <https://doi.org/10.1016/j.yexcr.2007.12.022>.

564 Pascucci L, Alessandri G, Dall'Aglia C, Mercati F, Coliolo P, Bazzucchi C, Dante S, Petrini  
 565 S, Curina G, Ceccarelli P (2014a) Membrane vesicles mediate pro-angiogenic activity of  
 566 equine adipose-derived mesenchymal stromal cells. *Vet J* 202:361-366.  
 567 <https://doi.org/10.1016/j.tvjl.2014.08.021>.

568 Pascucci L, Coccè V, Bonomi A, Ami D, Ceccarelli P, Ciusani E, Viganò L, Locatelli A,  
 569 Sisto F, Doglia SM, Parati E, Bernardo ME, Muraca M, Alessandri G, Bondiolotti G, Pessina  
 570 A (2014b) Paclitaxel is incorporated by mesenchymal stromal cells and released in exosomes  
 571 that inhibit in vitro tumor growth: a new approach for drug delivery. *J Control Release*  
 572 192:262-270. <https://doi.org/10.1016/j.jconrel.2014.07.042>.

573 Pascucci L, Dall'Aglia C, Bazzucchi C, Mercati F, Mancini MG, Pessina A, Alessandri G,  
 574 Giammarioli M, Dante S, Brunati G, Ceccarelli P (2015) Horse adipose-derived mesenchymal  
 575 stromal cells constitutively produce membrane vesicles: a morphological study. *Histol*  
 576 *Histopathol* 30:549-557. <https://doi.org/10.14670/HH-30.549>.

577 Pasquinelli G, Tazzari PL, Ricci F, Vaselli C, Buzzi M, Conte R, Orrico C, Foroni L, Stella  
 578 A, Alviano F, Bagnara GP, Lucarelli (2007) Ultrastructural characteristics of human  
 579 mesenchymal stromal (stem) cells derived from bone marrow and term placenta. *Ultrastr*  
 580 *Pathol* 31:23-31. <https://doi.org/10.1080/01913120601169477>.

581 Przybyt E, Krenning G, Brinker MG, Harmsen MC (2013) Adipose stromal cells primed with  
 582 hypoxia and inflammation enhance cardiomyocyte proliferation rate in vitro through STAT3  
 583 and Erk1/2. *J Transl Med* 11:39. <https://doi.org/10.1186/1479-5876-11-39>.

584 Rainaldi G, Pinto B, Piras A, Vatteroni L, Simi S, Citti L (1991) Reduction of proliferative  
 585 heterogeneity of CHEF18 Chinese hamster cell line during the progression toward  
 586 tumorigenicity. *In Vitro Cell Dev Biol* 27:949-952.

587 Rehman J, Traktuev D, Li J, Temm-Grove CJ, Bovenkerk JE, Pell CL, Johnstone BH,  
 588 Considine RV, March KL (2004) Secretion of angiogenic and antiapoptotic factors by human

589 adipose stromal cells. Circulation 109:1292-1298.  
590 <https://doi.org/10.1161/01.CIR.0000121425.42966.F1>.

591 Rossi B, Merlo B, Colleoni S, Iacono E, Tazzari PL, Ricci F, Lazzari G, Galli C (2014).  
592 Isolation and in vitro characterization of bovine amniotic fluid derived stem cells at different  
593 trimesters of pregnancy. Stem Cell Rev 10:712-724. [https://doi.org/10.1007/s12015-014-](https://doi.org/10.1007/s12015-014-9525-0)  
594 9525-0.

595 Schäffler A, Büchler C (2007) Concise review: adipose tissue-derived stromal cells - basic  
596 and clinical implications for novel cell-based therapies. Stem Cells 25:818-827.  
597 <https://doi.org/10.1634/stemcells.2006-0589>.

598 Schneider MR, Wolf E, Braun J, Kolb HJ, Adler H (2008) Canine embryo-derived stem cells  
599 and models for human diseases. Hum Mol Genet 17: R42-47.  
600 <https://doi.org/10.1093/hmg/ddn078>.

601 Seo MS, Jeong YH, Park JR, Park SB, Rho KH, Kim HS, Yu KR, Lee SH, Jung JW, Lee YS,  
602 Kang KS (2009) Isolation and characterization of canine umbilical cord blood-derived  
603 mesenchymal stem cells. J Vet Sci 10:181-187. <https://doi.org/10.4142/jvs.2009.10.3.181>.

604 Stubbs SL, Hsiao ST, Peshavariya HM, Lim SY, Disting GJ, Dilley RJ (2012) Hypoxic  
605 preconditioning enhances survival of human adipose-derived stem cells and conditions  
606 endothelial cells in vitro. Stem Cells Dev 21:1887-1896.  
607 <https://doi.org/10.1089/scd.2011.0289>.

608 Tapp H, Hanley EN Jr, Patt JC, Gruber HE (2009) Adipose-derived stem cells:  
609 characterization and current application in orthopaedic tissue repair. Exp Biol Med 234:1-9.  
610 <https://doi.org/10.3181/0805/MR-170>.

611 Tetta C, Ghigo E, Silengo L, Deregibus MC, Camussi G (2013) Extracellular vesicles as an  
612 emerging mechanism of cell-to-cell communication. Endocrine 44:11-19.  
613 <https://doi.org/10.1007/s12020-012-9839-0>.

614 Wang W, Itaka K, Ohba S, Nishiyama N, Chung UI, Yamasaki Y, Kataoka K (2009) 3D  
615 spheroid culture system on micropatterned substrates for improved differentiation efficiency  
616 of multipotent mesenchymal stem cells. *Biomaterials* 30:2705-2715.  
617 <https://doi.org/10.1016/j.biomaterials.2009.01.030>

618 Wenceslau CV, Miglino MA, Martins DS, Ambrosio CE, Lizier NF, Pignatari GC, Kerkis I  
619 (2011) Mesenchymal progenitor cells from canine fetal tissues: yolk sac, liver, and bone  
620 marrow. *Tissue Eng Part A* 17:2165-2176. <https://doi.org/10.1089/ten.tea.2010.0678>.

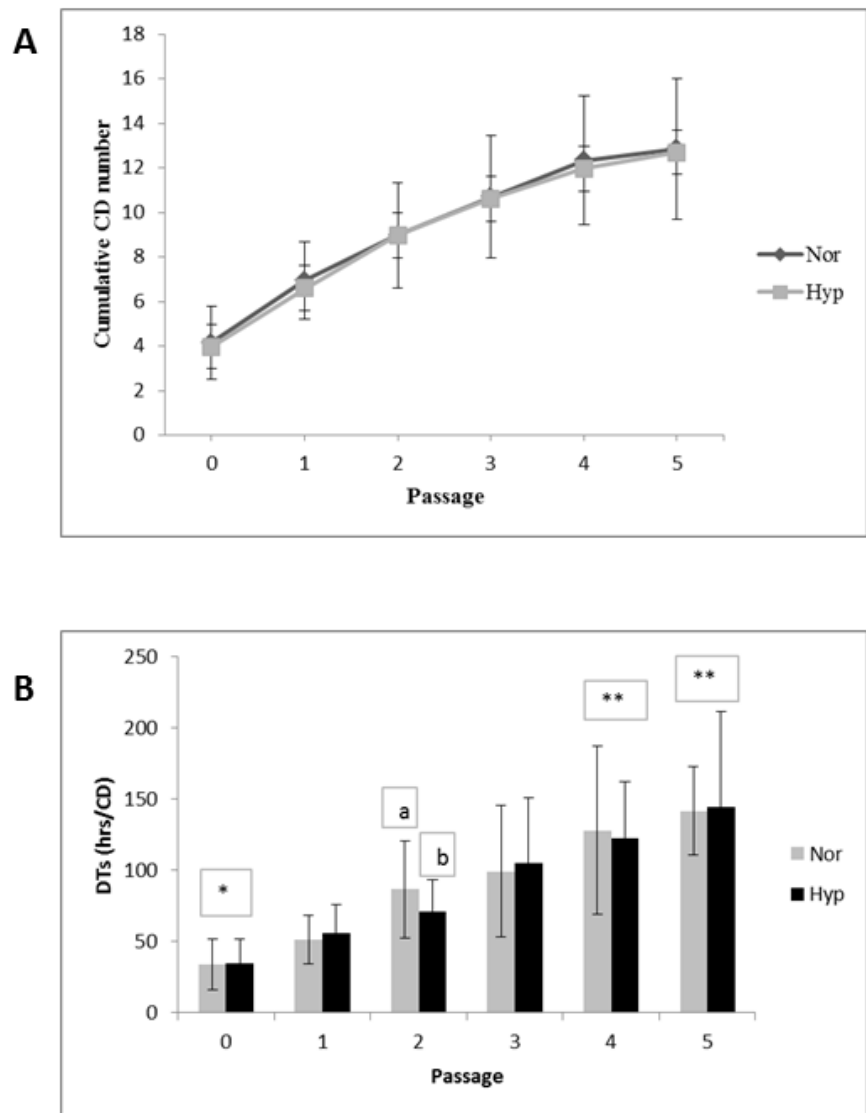
621 Yagi H, Soto-Gutierrez A, Parekkadan B, Kitagawa Y, Tompkins RG, Kobayashi N,  
622 Yarmush ML (2010) Mesenchymal stem cells: mechanisms of immunomodulation and  
623 homing. *Cell Transplant* 19:667-679. <https://doi.org/10.3727/096368910X508762>.

624 Zucconi E, Vieira NM, Bueno DF, Secco M, Jazedje T, Ambrosio CE, Passos-Bueno MR,  
625 Miglino MA, Zatz M (2010) Mesenchymal stem cells derived from canine umbilical cord  
626 vein-A novel source for cell therapy studies. *Stem Cells Dev* 19:395-402.  
627 <https://doi.org/10.1089/scd.2008.0314>.

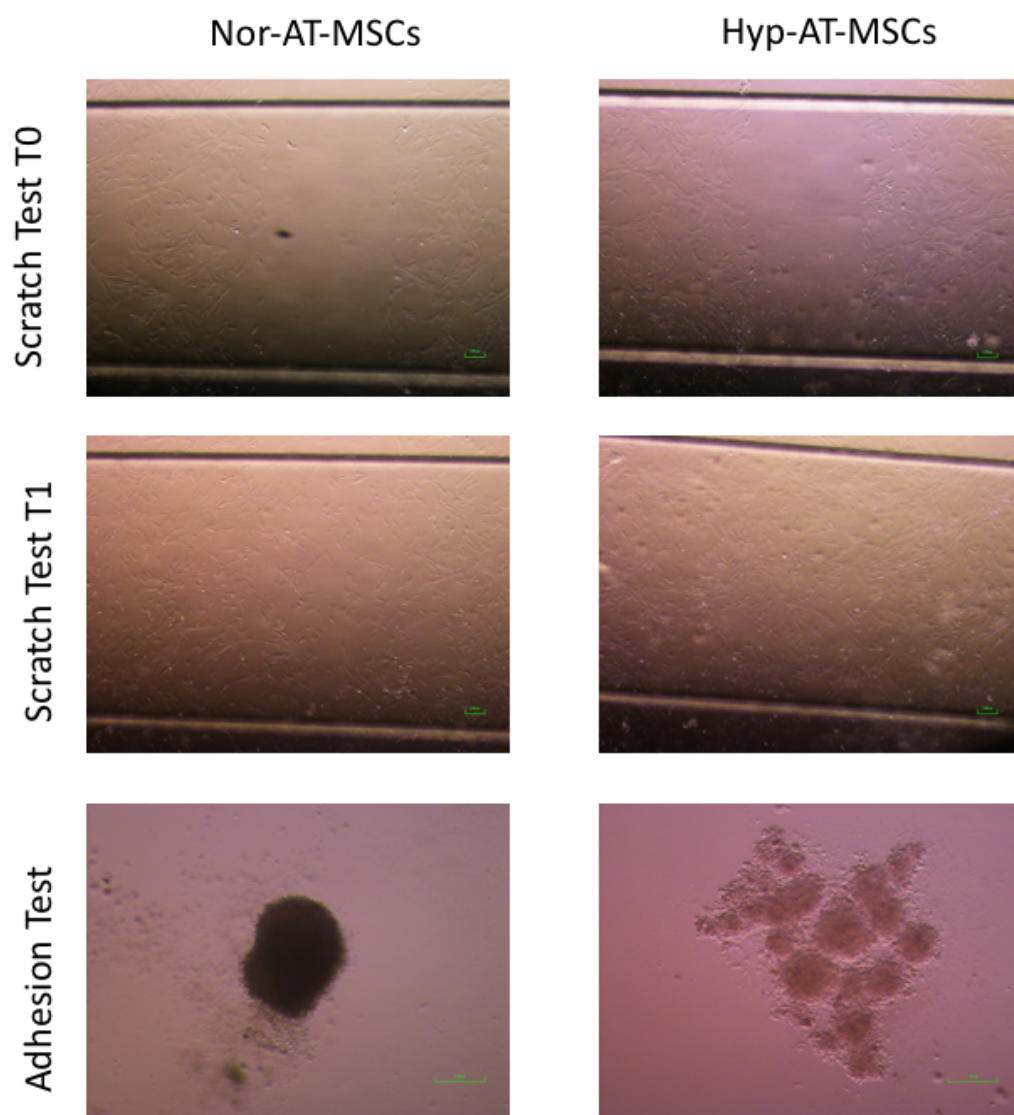
628

629 **Figure legends:**

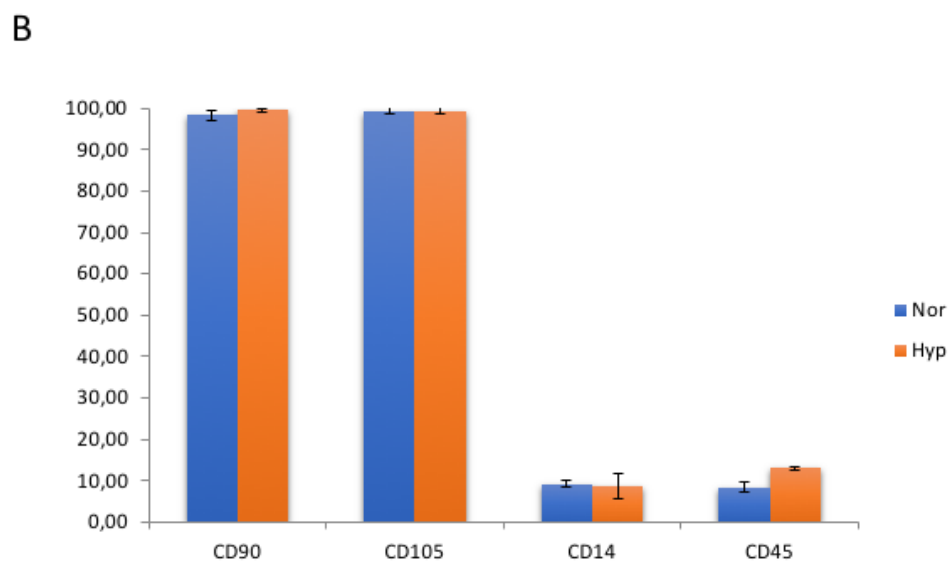
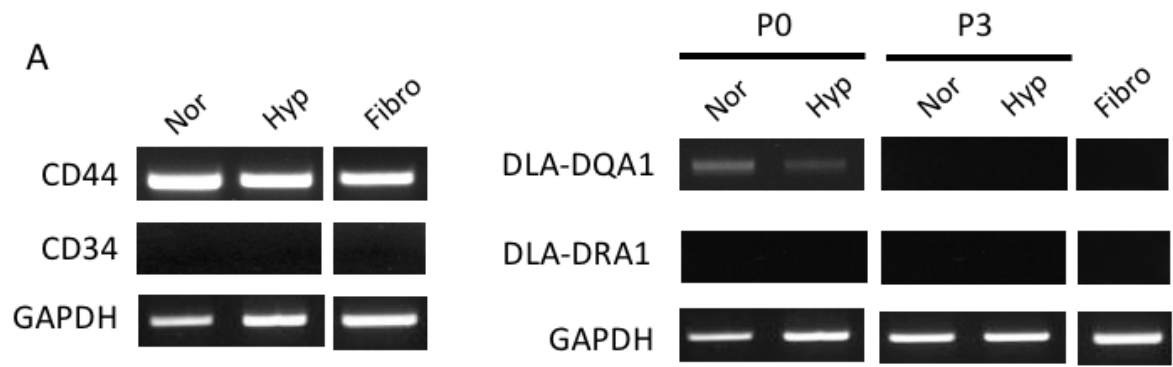
630 **Fig. 1.** Total Cell Doublings (A) and Doubling times (B) of Nor-AT-MSCs and Hyp-AT-  
631 MSCs over five passages of culture. A vs b, and \* vs \*\*:  $P < 0.05$ .



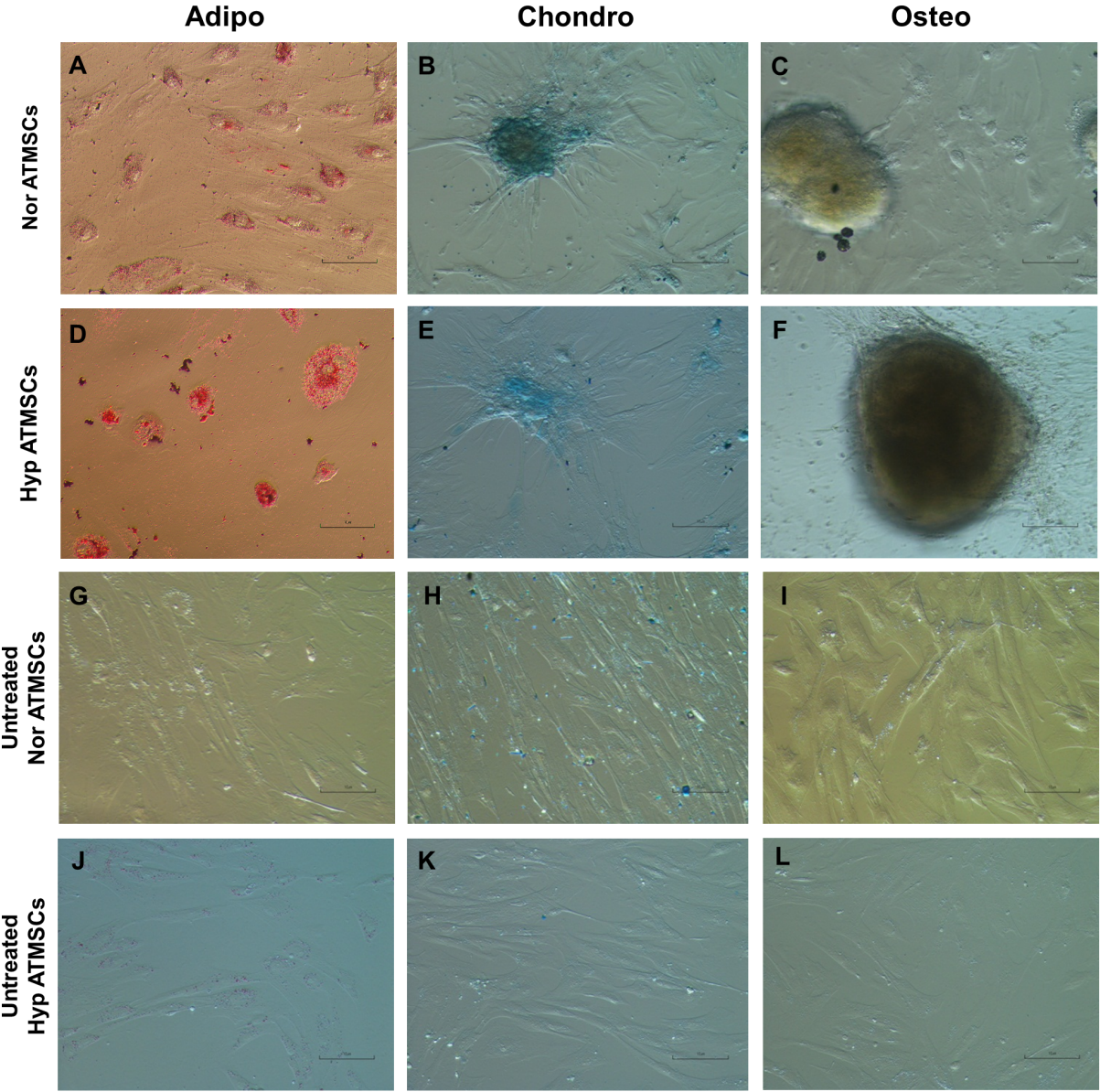
633 **Fig. 2.** A: Scratch assay on Nor-AT-MSCs and Hyp-AT-MSCs at T0 and after 24 h (T1) of  
634 cell growth (Magnification 4X, scale bar 100  $\mu$ m). B: Adhesion assay: Volume reconstruction  
635 and visualization of a Nor- and Hyp-AT-MSC spheroid, obtained after 48 h of hanging drop  
636 culture (Magnification 10x, scale bar 10 $\mu$ m).



638 **Fig. 3.** A: Representative RT-PCR analysis of gene expression in canine AT-MSCs cultured  
639 in different oxygen atmospheres. CD44, CD34 expression was evaluated on samples at P3  
640 whereas dog leukocytes antigens expression was studied both at P0 and at P3. B: Flow  
641 cytometric analysis. Nor-AT-MSCs and Hyp-AT-MSCs samples analyzed for different  
642 antigens expression (CD90, CD105, CD14, CD45) by FACS analysis.

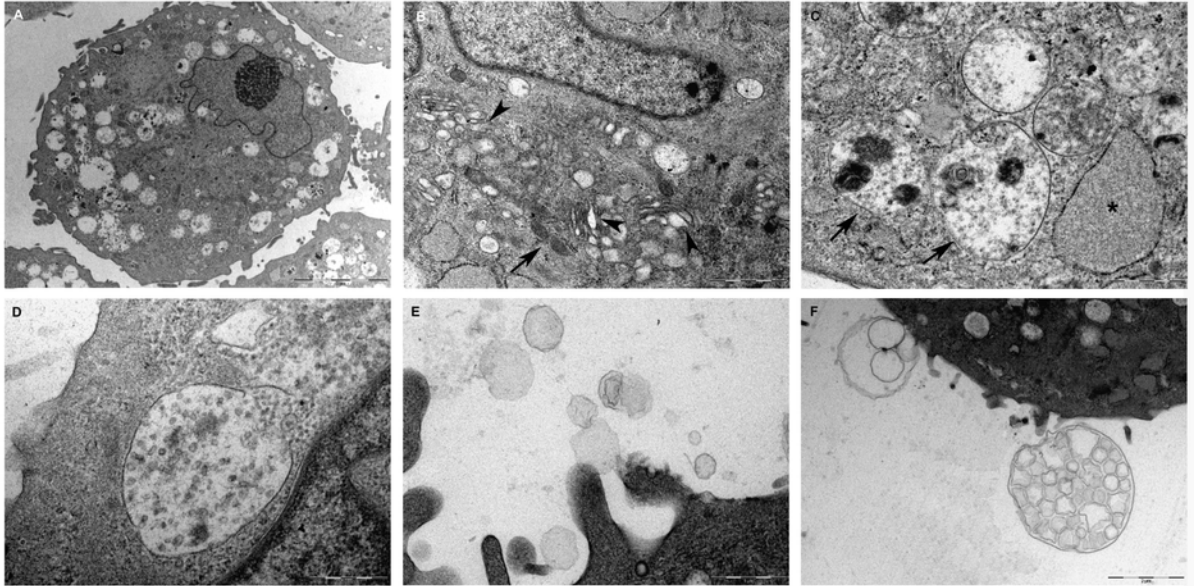


644 **Fig. 4.** Differentiation potential: Canine AT-MSCs cultured under adipogenic (A, D),  
 645 chondrogenic (B, E) and osteogenic (C, F) medium in normoxic and hypoxic conditions  
 646 respectively. G-L: Stained cells cultured in control medium. Magnification: 20X.

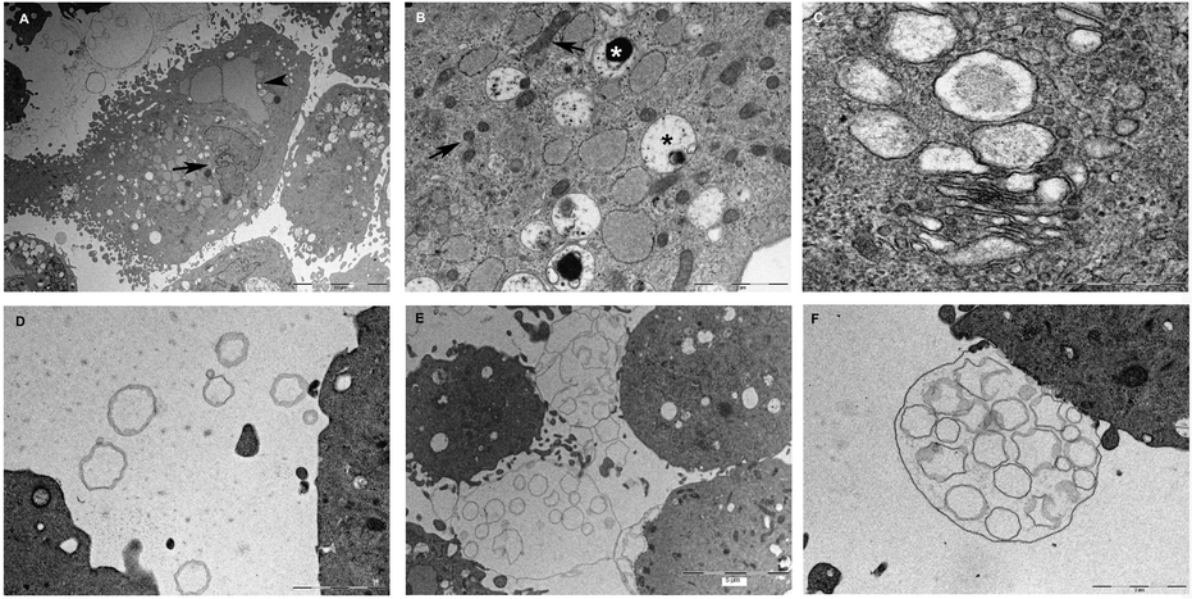


647  
 648 **Fig. 5.** Nor-AT-MSCs at TEM. **A.** At low magnification a single euchromatic irregular  
 649 nucleus containing a prominent nucleolus can be seen. Scale bar, 5 $\mu$ m. **B.** Note the abundance  
 650 of elongated mitochondria (arrow) and the well developed Golgi apparatus (arrowheads).  
 651 Scale bar 1  $\mu$ m. **C.** A group of endolysosomes with heterogeneous content can be observed  
 652 (arrows). Near them, a dilated RER cistern has been marked with an asterisk. Scale bar, 1 $\mu$ m.

653 **D.** A maturing MVB containing numerous endo-luminal vesicles. Scale bar, 500 nm. **E.**  
 654 Numerous vesicles of heterogeneous size can be observed in the extracellular space. Scale  
 655 bar, 1  $\mu$ m. **F.** Large complex electron-lucent vesicles budding from the cell surface and  
 656 containing smaller vesicles. Scale bar, 2  $\mu$ m.



657 **Fig. 6.** Hyp-AT-MSCs at TEM. **A.** Low magnification image showing a single euchromatic  
 658 nucleus (arrow) and cytoplasm containing a prominent RER with dilated cisternae  
 659 (arrowheads). Note the irregular cell profile determined by the presence of cytoplasmic  
 660 pseudopodial evaginations. Scale bar, 10  $\mu$ m. **B.** Cell cytoplasm with abundant mitochondria  
 661 (arrows), dilated RER and numerous MVB and endolysosomes (asterisks). Scale bar, 2  $\mu$ m.  
 662 **C.** Golgi apparatus is wide and well developed and is characterized by flattened cisternae,  
 663 transport vesicles, and large vacuoles, often filled with fine granular material. Scale bar, 500  
 664 nm. **D.** The image shows the presence of vesicles of heterogeneous dimensions located in the  
 665 extracellular space. Scale bar, 2  $\mu$ m. **E, F.** Note the presence of large vesicles shedding from  
 666 the cell surface and containing round-shaped smaller vesicles inside their lumen. Scale bar, 5  
 667  $\mu$ m and 2  $\mu$ m.  
 668



669

670

671 **Table 1:** Specific induction media compositions.

Adipogenic medium	Chondrogenic Medium	Osteogenic Medium
- DMEM/TCM199 - 10% FBS - 0.5 mM IBMX (removed after 3 days) - 1 µM DXM (removed after 6 days) - 10 µg/ml insulin - 0.1 mM indomethacin	- DMEM/TCM199 - 1% FBS - 6.25 µg/ml insulin - 50 nM AA2P - 0.1 µM DXM -10 ng/ml hTGF-β1	- DMEM/TCM199 - 10% FBS - 50 µM AA2P - 0.1 µM DXM - 10 mM BGP

672 IBMX: isobutylmethylxanthine, DXM: Dexamethasone, hTGF: human Transforming Growth

673 Factor, AA2P: Ascorbic Acid 2-Phosphate, BGP: Beta-Glycerophosphate

674

675 **Table 2:** Sequences of primers used for RT-PCR analysis

Gene	Primer sequences FW and RV	Amplicon (bp)	Reference
GAPDH	FW 5'-GGTCACCAGGGCTGCTTT-3' RV 5'-ATTTGATGTTGGCGGGAT-3'	209	(Jung et al. 2009)
CD44	FW 5'-GCCCTGAGCGTGGGCTTTGA-3' RV 5'-TCTGGCTGTAGCGGGTGCCA-3'	268	(Filioli Uranio et al. 2011)
CD34	FW 5'-GCCTGCTCAGTCTGCTGCCC-3' RV 5'-TGGTCCCAGGCGTTAGGGTGA-3'	255	(Filioli Uranio et al. 2011)
DLA-DRA1	FW 5'-CGCTCCAACCACACCCCGAA-3' RV 5'-GGCTGAGGGCAGGAAGGGGA-3'	246	(Filioli Uranio et al. 2011)
DLA-DQA1	FW 5'-GCACTGGGGCCTGGATGAGC-3' RV 5'-ACCTGAGCGCAGGCCTTGGA-3'	163	(Filioli Uranio et al. 2011)

676

677

678 **Table 3.** Primary antibodies and Isotype used for flow cytometry.

Markers	Ig
CD90 - PC5	IgG1
CD105 - PE	IgG2a
CD14 - PC5	IgG2a
CD45 - APC	IgG1
Isotype	
Isotype PC5	IgG2a
Isotype FITC	IgG1
Isotype PE	IgG1
Isotype APC	IgG1

679 Ig: immunoglobulin

680